Simulation of Jet Plume Impinging onto a Duct
닥트에 분사되는 제트플룸의 수치계산

홍승규* 이광섭* 백동기**

Abstract

Accurate simulation of jet plume exhausting into the open space as well as onto the opposing wall is of interest both numerically and physically; the latter, from a system designer's point of view. In the current work, Navier-Stokes computation is undertaken to capture the flow pattern of a supersonic jet impinging onto a rectangular duct which deflects the vertical jet horizontally. Of particular interest are the flow structure in the jet exhaust area, pressure pattern and the magnitude of pressure force at the bottom wall. Usefulness of present characteristic boundary condition applied at the exiting plane of the duct is demonstrated by capturing such complex flow structures for different lengths of the deflection duct.

1. INTRODUCTION

When a jet is exhausted into the free air, the jet interacts with the air and creates a complex flow pattern where the complexity depends on whether the jet is subsonic or supersonic. If the jet is supersonic, the jet exit pressure also determines the complexity of the flow structure which in the case of under-expanded jet reveals diamond-shaped shock cells with normal and oblique shocks. The intensity and the core length of the mixing region depends on whether the jet is either moderately or strongly expanded[1-3].

However, when a wall is placed blocking the exhaust jet, the interaction between the free jet and the wall further complicates the shock pattern, yielding a separation bubble in the stagnation area beneath the Mach disk and the plate shock.

Recently, Love et al.[4] conducted experimental study of jet impingement on heat transfer as a function of jet pressure and separation distance between the jet and the wall. Several experimental[2-4] and numerical works[5-7] have been reported on this jet impinging phenomenon; but, so far experimental works have led numerical computations because of difficulty in computing the shock/shock and shock/wall interaction flow fields.

In the current work, jet impingement from a circular jet onto a rectangular duct is simulated employing a computational procedure that adopts Roe's flux-difference splitting method in a modified form. The flow structure and the stability of the numerical solution are investigated for a few horizontal lengths of the deflection duct. Since the outflow boundary condition at the exit plane is not known, choice of exit condition would influence the solution. It was thought at the outset that application of characteristic boundary condition at the exit plane would result in a stable solution if the length of the duct is stretched adequately far enough. The present work subsequently shows that the stability of the numerical solution is not affected by merely lengthening the deflection duct. Rather, the distance between the jet exit plane and the opposing wall at the bottom is a major factor that influences the flow structure of the jet. In the present paper, however, attention is focused on the

* 정회원, 국방과학연구소(4-3-1)
** 공군사관학교 항공공학과

effect of lengthening the deflection duct on the flow structure as well as the numerical stability while the position of the jet is fixed.

2. PROBLEM DESCRIPTION

An axi-symmetric jet issuing from a circular nozzle is deflected horizontally through a rectangular duct as shown in Fig. 1 which is comprised of computational mesh at the surrounding wall. The jet impinges onto the bottom of the rectangular duct through a circular hole at the top of the duct. The bottom of the horizontal duct is $1.0D$ away vertically from the jet exit, where D represents the diameter of the cylindrical shroud that surrounds the exiting jet.

At the jet exit plane, the Mach number is 3.0, the static pressure is 14.1 psi and the Reynolds number is $7.1\text{x}10^6$ based on unit length(1 foot). It is thus weakly over-expended jet. The flow is also assumed to be turbulent and the turbulence model is called in the viscous wall region. Although the gas is in reality mixture of hot gases and particles, to simplify the computation, the gas is assumed to be an ideal one.

Among the questions raised are how the shock structure would be formed, where the highest pressure zone would occur, and more importantly whether it would remain steady. The steadiness of the numerical solution is examined closely, since the flow structure continues to change if the boundary condition is not settled properly. This fact led us to experiment with varying lengths of the horizontal duct.

3. NUMERICAL METHOD

The basic numerical algorithm follows conservative supra-characteristics method (CSCM) of Lombard et al.[8-11] and characteristic flux-difference splitting (CFDS) method of Yang et al.[12,13] which may be regarded as variants of Roe's flux-difference splitting (RFDS) method.[14,15] The present approach also adopts many ideas from flux-vector splitting formulations of Warming and Beam[16], Pulliam and Steger[17], Pulliam and Chaussee[18], among many others.

The governing Navier-Stokes equations employed in the generalized coordinate system, (ξ, η, ϕ), are expressed for the conservative variable vector as

$$J^{-1}\frac{\partial q}{\partial t}+\frac{\partial}{\partial \xi}(\hat{F}+\hat{F}_v)+\frac{\partial}{\partial \eta}(\hat{G}+\hat{G}_v)+\frac{\partial}{\partial \phi}(\hat{H}+\hat{H}_v)=0 \quad (1)$$

where $\hat{F}$, $\hat{G}$, and $\hat{H}$ are inviscid flux vectors, and $\hat{F}_v$, $\hat{G}_v$, $\hat{H}_v$ are viscous flux vectors. The inviscid fluxes are linearized and split for upwind discretizations by

$$\Delta_\xi F=\hat{A}\Delta q=(\hat{A}^+ + \hat{A}^-)\Delta q$$

and

$$\hat{A}^\pm = \overline{M}\,\overline{T}\,\overline{\Lambda}^\pm\,\overline{T}^{-1}\,\overline{M}^{-1} \quad (2)$$

yielding

$$J^{-1}\delta q+\hat{A}^+\nabla_\xi q+\hat{A}^-\Delta_\xi q+\hat{B}^+\nabla_\eta q+\hat{B}^-\Delta_\eta q+\hat{C}^+\nabla_\phi q+\hat{C}^-\Delta_\phi q+(\text{viscous terms})=0 \quad (3)$$

where $\delta q = q^{n+1}-q^n$ and the overbar, ( ), means the associated variable is spatial-averaged over the interval, [j,j+1]. $\overline{M}$ or $\overline{M}^{-1}$ is a transformation matrix between the conservative variable vector q and the primitive variable vector, say, $\tilde{q}$. $\overline{T}$ or $\overline{T}^{-1}$ is defined to be a transformation matrix between the primitive variable vector $\tilde{q}$ and the characteristic variable vector, say, $\tilde{\tilde{q}}$. The matrix product $\overline{M}\,\overline{T}$ or $\overline{T}^{-1}\,\overline{M}^{-1}$ represents transformation between q and $\tilde{\tilde{q}}$. Although finding $\overline{M}$ and $\overline{T}$ and their inverses requires many tedious algebraic steps, having $\hat{A}$ expressed in terms of $\overline{M}$ and $\overline{T}$ and their inverses

enables us to transform the conservative form of governing equations, Eq. (3), freely back to the characteristic form. It is easier to apply the characteristic boundary conditions when the equations are written in the characteristic form.

The viscous flux vectors associated with ξ, η and ϕ directions, respectively, can be related to the conservative vector q via

$$\hat{F}_v = A_v \triangle_\xi q, \quad \hat{G}_v = B_v \triangle_\eta q,$$
$$\hat{H}_v = C_v \triangle_\phi q \qquad (4)$$

For simplicity and practical purpose, ξ -direction viscous flux is neglected, and viscous coefficient matrices B_v and C_v are retained in the current formulation. Upwind flux-difference splitting for the inviscid fluxes and second-order central differencing for the viscous fluxes are then applied for discretizations. When the flow becomes turbulent, eddy viscosity is added to the laminar viscosity. Currently Baldwin-Lomax eddy viscosity model is utilized to account for flow turbulence. Solutions are then updated from q^n to q^{n+1} via implicit approximation in (η, ϕ)-plane and symmetric Gauss-Seidel relaxation for ξ -direction.

3.1 Boundary Conditions

Choice of proper boundary conditions is crucial for fast convergence. Application of characteristic boundary procedure is based upon a realization that there are five characteristics associated with the convective part of the Navier-Stokes equations. Especially for subsonic outflow boundaries, the first four characteristics propagate from the interior domain to the exit boundary and thus, their corresponding equations are retained as in the original Navier-Stokes equations. The fifth characteristics carries information from right to left toward the exit boundary from the outside of the computational domain. Since we do not know the value of it, nor its characteristic variable, it is customary to replace it by a suitable physical entity, say pressure p. Thus, for the fifth characteristic equation, the original characteristic equation, known as the P^- – equation, is replaced by an auxiliary equation condition, $\partial p / \partial t = 0$. This is in practice implemented through the change in the 5th row of T^{-1} by

$$\left[0, \ 0, \ 0, \ 0, \ \frac{1}{\gamma P} \right]$$

yielding

$$\delta \tilde{q} = T^{-1} \delta \hat{q} = \delta P / \gamma P = 0 \qquad (5)$$

At the wall, no-slip condition for velocity and adiabatic condition for temperature are imposed in the direction normal to the wall. In the symmetry plane, primitive variables are extrapolated from neighboring planes.

4. RESULTS AND DISCUSSIONS

The computational domain is divided into two regions: the jet plume area is discretized by a circular grid, and the rectangular duct area is represented by rectangular grid, as shown in Fig. 1. The grids with different topologies are overlapped by a grid cell where the two grids exchange data through interpolation. The circular grid consists of (j,k,l)=(33,35,37) for the symmetric half domain and shown in Fig. 1. The symmetry planes correspond to at l=1 and l=37 in the y-z space. Here the computational index (j,k,l) replaces the coordinate direction (ξ, η, ϕ). Along the jet centerline, at k=1 for all j's and l's of grid no. 1, the grid is singular and thus the flow variables are averaged from the neighboring points for each j. The second, rectangular grid which models the deflection duct is made of (46,40,69) for the standard case, where j=46 is at the open end of the duct.

In the beginning of computation, the flow structure was noticed to change continually as the iteration increased when

the boundary condition was extrapolated. This point was attributed partly to the nature of uncertain free boundary when the far-field boundary was not adequately distanced from the jet center and partly to unsettled pressure at the free boundary when the extrapolation method was applied. This problem was sought to be cured through numerical experimentation by placing the far-field boundary farther away from the jet center, extending the length of the duct by 1.0, 2.0, and 4.0D distance in the x direction in addition to what is shown in Fig. 1.

At the outset, the rest of the field except the nozzle exit plane was given a sea-level pressure and density as an initial condition. But the velocity field was inadvertently retained the same value as the jet exit velocity; which was unrealistically too high. Thus, this set of initial solution yielded continuously growing force exerted on the bottom wall. This problem disappeared when the initial velocity field was set to a smaller value, say, 0.1 times the jet exit velocity and the pressure, to the atmospheric pressure, coupled with imposition of characteristic method at the exit boundary. This stabilized the numerical solution even for the base case, which corresponds to that in Fig. 1 and is denoted in Fig. 2 as X=0D, meaning no eXtension. Then computations for the three other cases with longer deflection ducts were pursued to find out whether the results do show any difference in the flow structure. The pressure force integrated over the bottom wall area corresponding to that shown in Fig. 1, and later to that in Fig. 6, is plotted for four cases in Fig. 2 as a function of iteration number. The size of the extended duct length has been denoted by X=0, 1, 2, and 4D, for the four cases. The integrated pressure force settles toward a constant value after initial ups and downs after iter=2000 for all four curves. Presently solutions are taken at about iter=3500 to ensure the solutions have indeed reached a steady-state value.

Computational results thus obtained on Cray-YMP show that the shock is formed at the jet exit area and travels downstream at the outset, and that a shock shell bounded by a strong shear is formed gradually as the computational time increases. Mach disc is shown to form early in the computation and then reflected shock appears in the form of an oblique shock structure as shown in the yz mid-plane in Fig. 3 in terms of Mach contours. The reflected oblique shock creates a strongly sheared flow beneath the shock and makes the flow rotate, inducing a counter-rotating vortices above the stagnation region. Formation of such vortices due to jet shear layer is observed in Fig. 4 from velocity vectors. The wall pressure contours exhibit two high-pressure zones in Fig. 5 shown at the bottom of the deflection duct, displaying two concentric circles. The two pressure peaks occur because of oblique shocks, and this pattern has been observed in Ref.2 and by our in-house experiments repeatedly. In order to verify that what we have computed is within an experimental bound, an experiment is also concurrently carried out by our internal working group. A model is prepared and total force is measured impacting the bottom wall of Fig. 5. Wall pressure values are also recorded along z-coordinate and x-coordinate locations at the bottom wall of Fig. 5. The computed total force matches within 5 percent of the measured force and predicted wall pressure distributions match very closely with measured values. Figure 6 shows comparison between the computed and measured pressure along the bottom line of Fig. 3. The scales in the figure are arbitrary and z=0 indicates the middle point between the two parallel walls. Mach contours are also presented in Fig. 7 in xy-plane along the mid-plane(z=0), showing a pocket of shock shell.

It is important to point out that similar results are obtained for the other three cases with longer duct size. In order to show independence of shock structure on the duct lengths, it is sufficient to present Mach contours in the cases of X=1D, 2D and 4D in the middle xy-plane in Figs. 8, 9 and 10

respectively. They are comparable to Fig. 7 and display a similar core structure even if the duct length has been extended due to the supersonic nature of the current jet flow. This in turn proves that current method of computing jet impingement process serves as a well-established viable tool in designing a flame deflector and is also shown to yield a stable numerical solution as well as the flow structure that is backed up by experiments.

5. CONCLUDING REMARKS

Objectives of present work were to uncover details of jet impingement process in the presence of wall. Emphasis has been placed on testing the effect of the duct length on obtaining a stable numerical solution. The current study reveals that the flow structure retains basically the same pattern even if the length of the duct is lengthened and that merely lengthening the duct length alone does not overcome the uncertainty associated with the outflow boundary condition.

Verification of accuracy of current work was carried out independently through an experimental work and comparisons between the measured and computed pressure are quite satisfactory.

ACKNOWLEDGEMENTS

Authors express their thanks to the experimental group (4-3-4) that carried out the quoted experiment and also to computer support group at ADD for allowing us a generous disk quota on Cray-YMP.

REFERENCES

1. Liepmann, H. W. and Roshko, A., Elements of Gasdynamics, Wiley and Sons, Inc., New York, 1957, p. 128.

2. Donaldson, C. and Snedecker, "A study of free jet impingement. Part 1. Mean properties of free and impinging jets," J. Fluid Mech., Vol. 45, 1971, pp. 281-319.

3. Lamont, P. J. and Hunt, B. L., "The impingement of underexpanded, axisymmetric jets on perpendicular and inclined flat plates," J. Fluid Mech., Vol. 100, 1980, pp. 471-511.

4. Love, J. G., Stuerman M. T., Murthy, S.N.B. et al., "Experimental Investigations of the Heat Transfer Characteristics of Impinging Jets," AIAA 94-0262, Reno, January 1994.

5. Tsuboi, N., et al., "Numerical Simulation of Supersonic Jet Impingement on a Plate," 5th CFD Conference, Tokyo, Japan, Dec. 1991, pp. 155-158.

6. Kim, K. H., "Numerical Analysis of Supersonic Jets Impinging into an Obstacle," Ph. D. Thesis, Korea Advanced Institute of Science and Technology, Taejon, Korea, May 1993.

7. Hong, S. K. and Jeon, H. J., "Computational Study of Supersonic Jet Impingement on Flat and Complex Surfaces," AIAA-94-2326, 25th Fluid Dynamics Conferences, June 1994, Colorado Springs.

8. Lombard, C. K., Oliger, J., Yang, J. Y. and Davy, W. C., "Conservative Supra-Characteristics Method for Splitting the Hyperbolic Systems of Gasdynamics with Computed Boundaries for Real and Perfect Gases," AIAA-82-0837, June 1982.

9. Lombard, C. K., Oliger, J., Yang, J. Y. "A Natural Conservative Flux Difference Splitting for the Hyperbolic Systems of Gasdynamics," AIAA-82-0976, June 1982.

10. Lombard, C. K., et al., "Multi-Dimensional Formulation of CSCM - An Upwind Flux Difference Eigenvector Split Method for the Compressible Navier-Stokes Equations", AIAA-83-1895, AIAA 6th CFD Conference, July 1983.

11. Hong, S. K., Bardina, J., Lombard, C. K., Wang, D. and Codding, W., "A Matrix of 3-D Turbulent CFD Solutions for JI Control with Interacting Lateral and Attitude Thrusters,"AIAA 91-2099, Sacramento, June 1991.

12. Yang, J. Y., "A Characteristic Flux Difference Splitting Method for Hyperbolic Systems of Conservation Laws," Ph.D. Thesis, Stanford University, June 1982.

13. Yang. J. Y. and Lombard, C. K., "A Characteristic Flux Difference Splitting for the Hyperbolic Conservation Laws of Inviscid

Gasdynamics," AIAA-83-0040, Reno, Jan 1983.

14. Roe, P. L., "The use of Riemann problem in finite difference schemes," Lecture Notes in Physics, Vol. 141, 1981, pp. 354-359, Berlin, Springer Verlag.

15. Roe, P. L., "Approximate Riemann solvers, parameter vectors and difference scheme," J. of Computational Physics, 43, 1981, pp. 357-372.

16. Warming, R.F. and Beam, R. M.,"On the Construction of Implicit Factored Schemes for Conservation Laws," Computational Fluid Dynamics, SIAM-AMS Proceedings, Vol. 11, 1978, pp.85-127.

17. Pulliam, T. H. and Steger, J. L. "On Implicit Finite Difference Simulations of Three-Dimensional Flows," AIAA-78-10, January 1978.

18. Pulliam, T. H. and Chaussee, D. S., "A Diagonal Form of an Implicit Approximate-Factorization Algorithm,", Journal of Computational Physics, Vol. 39, pp.347-363, 1981.

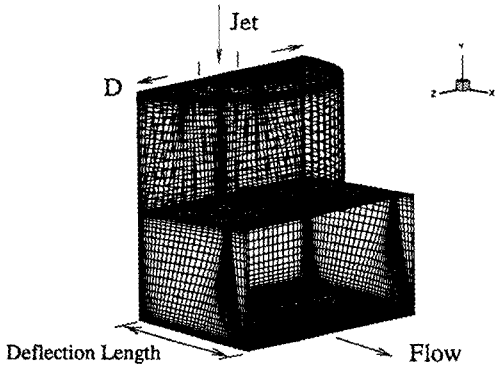

Fig.1 Grid system at the wall boundaries.

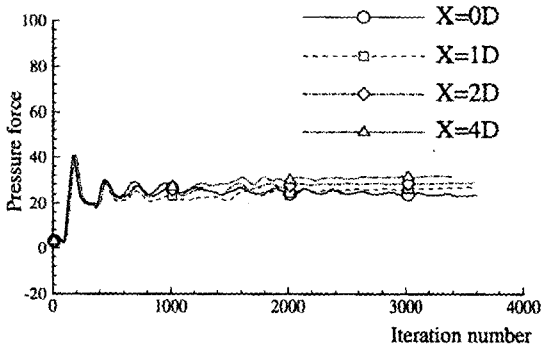

Fig.2 Total pressure force as a function of iteration.

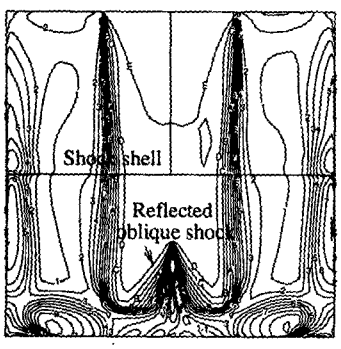

Level	Mach
E	2.78
D	2.58
C	2.38
B	2.19
A	1.99
9	1.79
8	1.59
7	1.39
6	1.19
5	0.99
4	0.79
3	0.60
2	0.40
1	0.20

Fig.3 Mach contours in yz-symmetry plane.

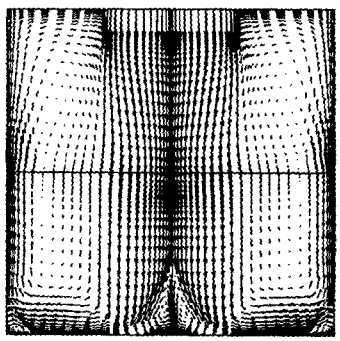

Fig.4 Velocity vectors in yz-symmetry plane.

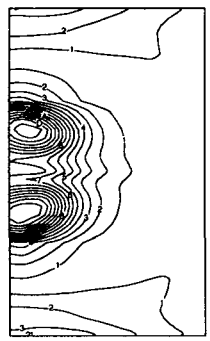

Fig.5 Wall pressure contours in xz bottom plane.

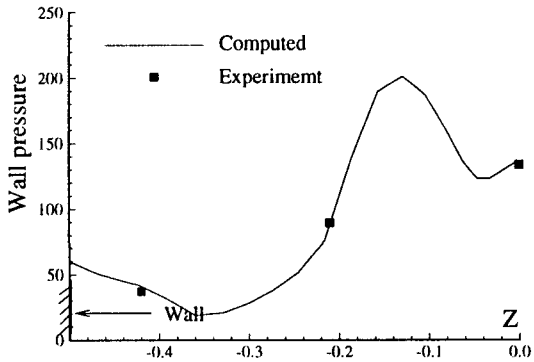

Fig.6 Wall pressure distribution along yz-symmetry plane.

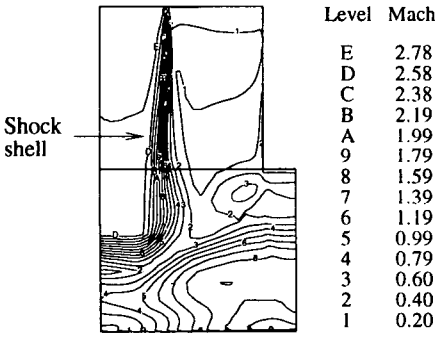

Fig.7 Mach contours in xy plane through middle z.(X=0.0D)

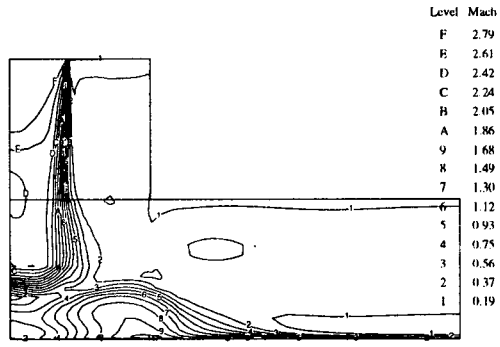

Fig.8 Mach contours in xy plane through middle z(X=1.0D)

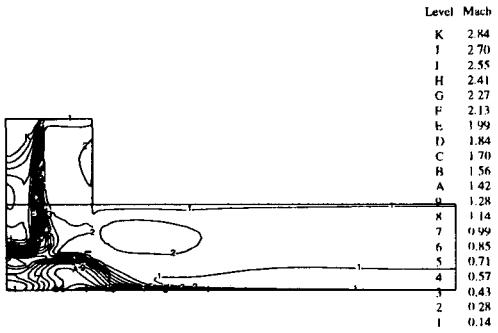

Fig. 9 Mach contours in xy plane through middle z(X=2.0D)

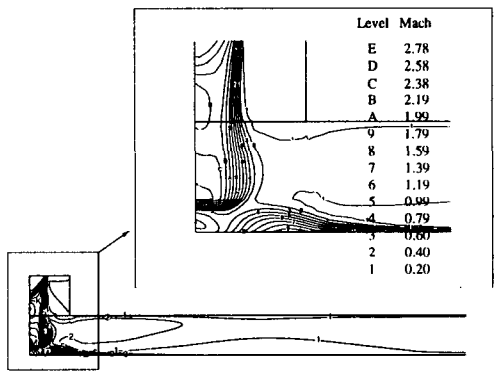

Fig.10 Mach contours in xy plane through middle z(X=4.0D).